Regional Ecosystem-Atmosphere CO_2 Exchange Via Atmospheric Budgets

Principal Investigators: Kenneth J. Davis and Scott J. Richardson

September 2002 – August 2005

Department of Meteorology
The Pennsylvania State University
503 Walker Building
University Park, PA 16802

Final Report for DE-FG02-02ER63475

1. Introduction

Current techniques for measuring the exchange of carbon dioxide between the earth's surface and the atmosphere yield results representing disparate spatial scales. Tower-based eddy covariance measurements provide estimates of net ecosystem-atmosphere exchange (NEE) at scales ranging from 0.01 km^2 to 10 km^2 (e.g., Wofsy et al., 1993; Davis et al., 2003), and ecological inventories are typically conducted on plots with areas of many square meters. Whereas global CO_2 mixing ratio measurements provide the means to infer (by inversion of atmospheric tracer transport) NEE at hemispheric and perhaps continental scales (e.g., Enting et al., 1995; Fan et al., 1998; Rayner et al., 1999; Bousquet et al., 2000; Gurney et al., 2002). Estimating carbon fluxes using both methods has been critical to elucidating the processes that govern the terrestrial carbon cycle: tower-based methods provide an understanding of specific mechanisms that govern carbon fluxes in particular ecosystems (e.g., Goulden et al., 1998; Baldocchi et al., 2001), while inverse estimates of NEE integrate the effects of all the physical, biogeochemical, and anthropogenic processes operating over large scales.

The carbon cycle research community has had limited success to date, however, in achieving understanding of the mechanisms governing terrestrial NEE at regional to continental scales given the gap in spatial scales represented by the various measurement methods. Existing intercomparisons have largely been limited to continental scales (e.g. Pacala et al., 2001; Janssens et al., 2003) and have large uncertainty, hence limited ability to date to test mechanistic hypotheses. Regional flux estimation by upscaling flux or inventory based estimates while simultaneously performing regional atmospheric inversions may yield more precise comparisons grounded in process-based understanding, and at scales clearly relevant to the global carbon balance. Short-term experiments, covering time-spans of weeks and using airborne CO_2 measurements, have yielded promising results (Gerbig et al., 2003; Matross et al., 2006). Longer-term field efforts based on a mixture of atmospheric observing platforms are underway (e.g. Denning et al., 2005). This study is an example of one such effort.

Inverse analyses of continental to global scale surface-atmosphere CO_2 exchange has typically been based on interpretation of very subtle spatial patterns in CO_2 mixing ratios in the monthly mean (e.g. Gurney et al., 2002). To obtain "representative" concentration measurements, samples are collected far from local sources and sinks, mostly in the remote marine boundary layer (Masarie and Tans, 1995). Differences among sites are very small, so the measurements must be very precise, and intercalibration among different sites and laboratories is crucial (Masarie et al., 2001). Differences in annual mean concentrations between stations in the Atlantic and the Pacific, for example, are less than 1.0 ppm, and estimates of the overall sink in North America are very sensitive to errors on the order of 0.2 ppm in this difference.

Network optimization studies have consistently suggested that more accurate estimation of continental sources and sinks could be achieved by sampling the continental atmosphere (Rayner et al., 1996; Gloor et al., 2000). The concentration field is much more variable over the continents than in the marine boundary layer. Traditional inversion methodology regards these variations as "noise" and seeks to interpret smoother time-averaged spatial patterns. Utilizing the information contained in this variability, however, will required appropriate measurement and modeling of the associated atmospheric concentration and transport field. Weekly flask samples and coarse-resolution global models, for example, are unlikely to take full advantage of continental boundary layer observations.

An emerging idea in the carbon cycle science community is that there may be much more information content in the high-time frequency variations in CO_2 in the continental boundary layer than in the time mean spatial patterns. This approach seeks to observe and interpret these variations rather than smooth them by time averaging, turning the "noise" into "signal." Variations on hourly to synoptic time scales of 10−20 ppm are not unusual in data collected at the WLEF-TV tower in northern Wisconsin (Davis et al., 2003; Hurwitz et al., 2004). These variations are more than an order of magnitude stronger than those interpreted by global to continental inverse modeling of seasonally-averaged observations, and appear to be systematically related to particular trajectories, based on their association with wind directions and frontal passages (Hurwitz et al., 2004; Wang et al., in press).

Inversions of atmospheric CO_2 mixing ratio measurements to determine CO_2 sources and sinks are typically limited to coarse spatial and temporal resolution. This limits our ability to evaluate efforts to upscale chamber- and stand-level CO_2 flux measurements to regional scales, where coherent climate and ecosystem mechanisms govern the carbon cycle. As a first step towards the goal of implementing atmospheric budget or inversion methodology on a regional scale, a network of five relatively inexpensive CO_2 mixing ratio measurement systems was deployed on towers in northern Wisconsin. Four systems were distributed on a circle of roughly 150-km radius, surrounding one centrally located system at the WLEF tower near Park Falls, WI. All measurements were taken at a height of 76 m AGL. The systems used single-cell infrared CO_2 analyzers (Licor, model LI-820) rather than the siginificantly more costly two-cell models, and were calibrated every two hours using four samples known to within ± 0.2 ppm CO_2. Tests prior to deployment in which the systems sampled the same air indicate the precision of the systems to be better than ± 0.3 ppm and the accuracy, based on the difference between the daily mean of one system and a co-located NOAA-ESRL system, is consistently better than ± 0.3 ppm.

The utility of the network is demonstrated in two ways. We interpret regional CO_2 differences using a Lagrangian parcel approach. The difference in the CO_2 mixing ratios across the network is at least 2−3 ppm, which is large compared to the accuracy and precision of the systems. Fluxes estimated assuming Lagrangian parcel transport are of the same sign and magnitude as eddy-covariance flux measurements at the centrally-located WLEF tower. These results indicate that the network will be useful in a full inversion model. Second, we present a case study involving a frontal passage through the region. The progression of a front across the network is evident; changes as large as four ppm in one minute are captured. Through this project, development of the modeling framework to analyze CO2 tower measurements and to estimate regional CO2 fluxes, using the CSU Regional Atmospheric Modeling System (RAMS), the Lagrangian Particle Dispersion Model (LPDM), an influence function approach and an inversion method, has continued. Influence functions from the modeling results are used to determine source regions for the towers. The influence functions are combined with satellite vegetation observations to interpret the observed trends in CO_2 concentration. Full inversions will combine these elements in a more formal analytic framework.

2. Experimental Design

2.1 Study sites

Figure 1. Map of the sites included in the ChEAS regional network of CO_2 mixing ratio measurements in northern Wisconsin. The measurement height for the Brule, Bayfield, WLEF, Fence, and Wittenberg sites is 76 m, whereas the measurement height for the Sylvania site is 36 m. The Sylvania dataset was collected using field-calibrated standards and may have an offset of 0.5−1.0 ppm. In addition to the data presented in this paper, the CO_2 mixing ratio is also measured by NOAA-ESRL at 11, 30, 76, 122, 244, and 396 m at the WLEF site for comparison. Data from the Wheeler site was not used due to system unreliability.

Fig. 1 shows the location of the four towers around the central site at the WLEF tower located near Park Falls, WI; the circle is 150 km in radius centered on the WLEF tower. The tower spacing – outer edge to central WLEF site – is approximately 8−12 hours of advection time in the boundary layer in order to be optimal for measuring fluxes integrated over the course of the day. Measurements of CO_2 mixing ratios (Bakwin et al., 1998) have been made at the WLEF site since 1994 and locating one of the five CO_2 systems at the WLEF tower provided a direct comparison with a known measurement and served as an indicator of measurement uncertainty. The remaining four sites are shown in Fig. 1 and are located near Fence, Wittenberg, Brule, and Bayfield, WI. An additional site, in Wheeler, WI, was planned but the data are not used because of system errors. All systems sampled air from 76 m agl on communications towers. CO_2 concentration data from the Sylvania Wilderness tower supplemented the data from the five primary sites for the frontal passage case study. The CO_2 concentration measurement system at this site is similar to that described by Bakwin et al. (1998). The system is calibrated every four hours using three field-calibrated standards known to approximately 0.5−1.0 ppm CO_2; thus the absolute accuracy may be offset from the five primary systems.

The towers are located within the Chequamegon Ecosystem-Atmosphere Study (http://**www.cheas.psu.edu**) area, which has been the subject of intensive multi-investigator studies of forest-atmosphere cycling of carbon and water (e.g., Baker et al., 2003; Cook et al., 2004; Bresee et al., 2004; Mackay et al., in press). The region primarily consists of dense temperate forests and lowland wetlands. The population density of the area is low so there is minimal local contamination of the CO_2 mixing ratio and flux signals from anthropogenic emissions. There are, however, large population centers located outside of the ring, and these population centers are occasionaly downwind of the towers. Agricultural land borders to the south, and the Great Lakes to the north and east. .

2.2 Measurement system description

The systems are similar in concept to those described by Zhao et al., (1997), and Bakwin et al., (1998). Changes, made in collaboration with B. Stephens and A. Watt of NCAR-ATD, lowered the cost of the systems to facilitate deployment of a network of several systems while maintaining high precision and accuracy. Fig. 2 is a schematic of the sampling and measurement systems used at each of the sites. On each tower, tubing (1/4 inch (6.4 mm) outer diameter, Synflex [formerly known as Dekoron] type 1300) was mounted with an inlet at 76 m above the ground. Air was drawn down to ground level using a DC brushless pump. Upstream of the pump the air was filtered using a 1-μm filter for dust and downstream of the pump a particulate filter was used to extract liquid water. The flow rate was adjusted to be 150 cc min^{-1} using a pressure relief valve. A multiport valve was used to select between the sample and calibration gases. A Nafion drier (Permapure, model MD-110-144) with nitrogen counterflow was used to dry the sample air and to moisten the calibration gases (the field standards purchased from Scott-Marrin Inc. had << 10 ppm H_2O). The CO_2 levels were measured using IR absorption spectroscopy (LICOR, model LI-820). The temperature and relative humidity of the air sample and calibration gases were monitored. A data logger (Campbell Scientific, model CR10X) was used for data acquisition and system control.

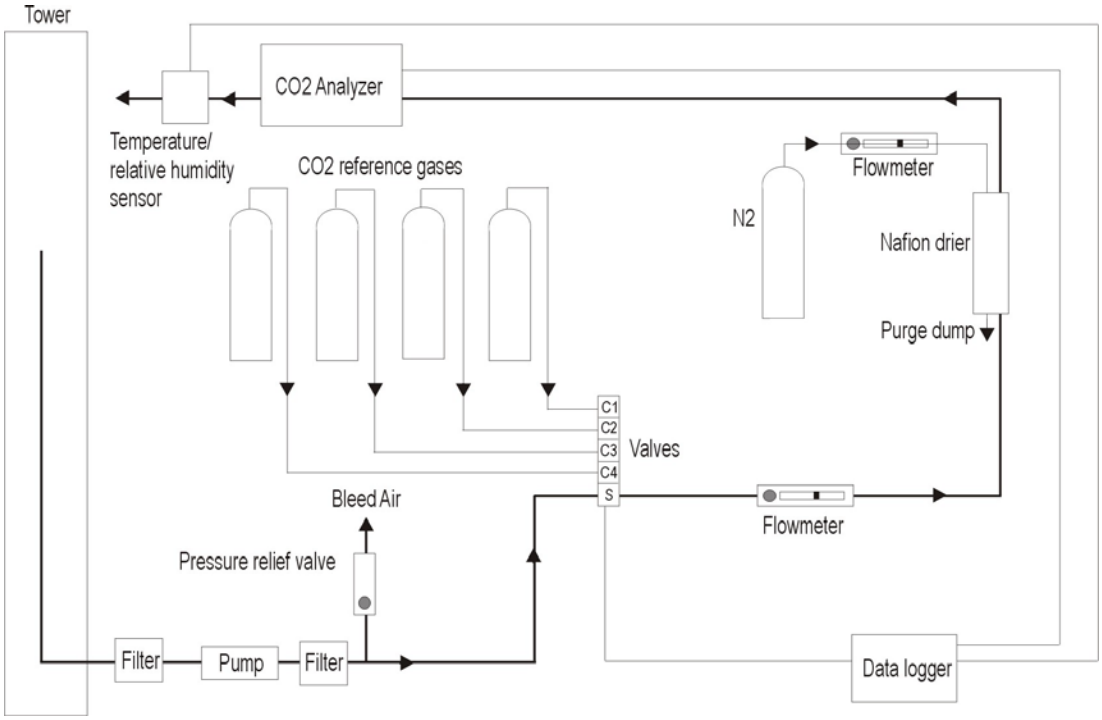

Figure 2. A schematic of the CO_2 mixing ratio measurement system.

While accuracy and precison are very important to this study, fast time response of the CO_2 mixing ratio sensor is not required. The single-cell LI-820 sensor was chosen based on its relatively low cost compared to the two-cell LI-7000. Although peak-to-peak noise for 1-s samples is 3 ppm for the LI-820, compared to 0.3 ppm for the LI-7000, the noise can be reduced to 0.2 ppm by averaging for 5 min because tests showed that the noise is random. Comparisons between the performance of the LI-820 and LI-7000 in laboratory tests are shown in Section 2.4 and comparisons between a PSU system using an LI-820 and an independent NOAA-ESRL system using a (two-cell) LI-6251 are shown in Section 2.5.

2.3 Calibration

Frequent calibration is necessary to characterize and remove the nonlinear response of the CO_2 sensor to changes in temperature and pressure. Four standards, hereafter referred to as "field standards", containing approximately 330, 360, 390, and 420 ppm CO_2 in air were analyzed for 8 min each during each calibration sequence. These four known values were used to develop a second-order linear regression between the LI-820 voltage output and CO_2 mixing ratio. Calibration sequences were performed every 2 hours throughout the deployment.

The field standards were purchased from Scott-Marrin Inc. and characterized in our laboratory following the general methods and practices of NOAA-ESRL (Kitzis and Zhao, 1999). This included the use of seven calibrated standard reference gases which were purchased from NOAA-ESRL and used as laboratory calibration standards. The accuracy of the calibrations performed at the PSU calibration facility were evaluated because the accuracy of the field standards directly affects the accuracy of the CO_2 mixing ratio measurements through the accuracy of the linear regression. One method used to evaluate the repeatability of the calibrations was to include the same field standard tank in each calibration sequence. One tank was calibrated 35 times and the average value was 367.63 ppm with a standard deviation of 0.02 ppm. Because only four of the seven laboratory standards were used in the calibration process, the remaining three NOAA-ESRL calibrated tanks were periodically tested as if they were unknowns. This procedure was performed several times and in every case the calibrated value was within 0.05 ppm of the NOAA-ESRL value. The final test of the calibration facility was to calibrate a roving standard as part of the 4th World

Meteorological Organization round-robin reference gas intercomparison (Group 2); the results of these comparisons have not yet been released. Based on these tests the calibration absolute accuracy of the field standards is expected to be better than 0.1 ppm.

2.4 System precision

Before deploying the five CO_2 systems, their precision was tested by sampling the same air. All systems sampled outdoor air in parallel from a four-liter mixing volume which had a fan actively circulating the air. While it is possible to set up a laboratory test with all systems using the same field standards, each system used its own set in order to more accurately measure the precision in the field which includes errors in the field standards. An LI-7000 was connected in series with one of the five systems to reveal any possible systematic bias associated with the use of the LI-820. Fig. 3 shows the $[CO_2]$ measured by all five systems, as well as that measured by the LI-7000. The maximum difference from the mean for all the systems is generally less than ± 0.3 ppm throughout the test period. The overall differences from the mean during the test were +0.02, −0.17, −0.09, +0.12, +0.10 ppm for the five systems, and +0.06 ppm for the LI-7000, suggesting no problems were associated with using the LI-820 rather than the LI-7000 for this type of measurement. Since these systems are not temperature controlled (although the LI-820 does actively control the temperature of the sensor itself to about 50ºC), differences in temperature between systems in the field that occur on time scales less than the calibration frequency may contribute additional error. Although the flow rate (and thus the pressure) were controlled somewhat in the systems, pressure differences in the field on time scales less than the calibration time scale may also contribute to additional error. Errors due to differences in pressure and temperature on time scales larger than the calibration time scale, however, should be eliminated by calibration.

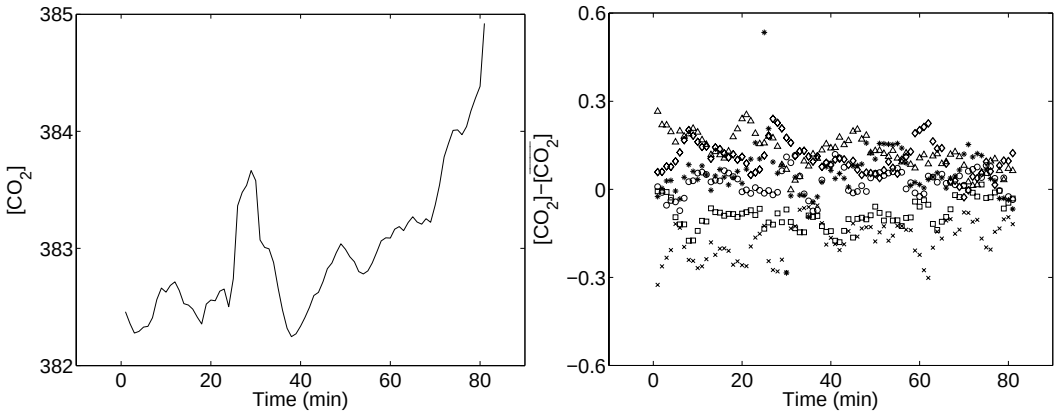

Figure 3. a) Mean CO_2 mixing ratio as measured by five systems using separate calibration tanks and sampling the same outdoor air. b) Difference from the mean CO_2 mixing ratio of five systems using separate calibration tanks (open symbols and x symbol) and an LI-7000 (* symbol) sampling the same outdoor air.

2.5 PSU vs. NOAA-ESRL CO_2 concentration measurement comparison

As a further means to evaluate the performance of the systems, one system was deployed at the WLEF tower near Park Falls, WI, (Bakwin et al. 1998) where a NOAA-ESRL system also measured CO_2 mixing ratio. The PSU system sample line branched off from the NOAA-ESRL system 76-m sample line at the base of the tower to ensure that both systems were sampling identical air. Because of different tubing lengths and flows between the two systems, the timing was likely to be slightly different for the two systems. The NOAA-ESRL system sampled at the 76-m tower level for 2 min every 12 min. Because of the time required for the sample line to flush, the final 30 s of data from each 2 minute sample were used to calculate the average CO_2 mixing ratio. The PSU data were averaged and saved every minute in the field. Thus the 1-min average of the PSU data corresponding as closely as possible to to the NOAA-ESRL data considering the difference in lag times was used in the comparison; this happened to be the minute with the

closest time stamp to that of the NOAA-ESRL data. The NOAA-ESRL and PSU systems had independent filtering and, more importantly, drying, with the NOAA-ESRL system using a refrigerated, continuously purged liquid water trap, followed by a Nafion drier (Bakwin et al. 1998). A Hygrometrix relative humidity sensor was used to monitor residual moisture levels. In addition, the NOAA-ESRL system used a LI-6251 further testing for possible problems associated with the use of the LI-820 in the PSU systems. The overall trends in CO_2 mixing ratio measurements by the two systems at the WLEF tower during April–August 2004 are shown in Fig. 4. Leaf-out, after which the CO_2 mixing ratio is more variable, occurred around 10 May (Day 131) in 2004, with full expansion around 11 June (Day 163) (B. Cook, personal communication). There are three periods during which both the PSU and NOAA-ESRL systems were operational (noting that the PSU and NOAA-ESRL system each had one extended (~20 days) inoperable period) and the difference between the CO_2 mixing ratio measured by the two systems for these periods is shown in Fig. 5a. The estimated uncertainty of the NOAA-ESRL system, including uncertainty in the calibration scale, uncertainty due to drift in the CO_2 analyzer baseline and sensitivity between calibrations, uncertainty due to lack of equilibration of air samples or standards, and uncertainty due to real natural variability of the CO_2 abundance during the measurement period, and calculated such that the actual value should be within one times the uncertainty estimate of the measured value 67% of the time, is also shown (A. Andrews, personal communication). Overall for the three periods, the PSU value is within one times the uncertainty estimate of the NOAA-ESRL value for 57% of the values. The average uncertainty estimate is 0.29 ppm, but there are several points with uncertainties of 1−2 ppm (one point is even larger than 5 ppm) and these points often correspond to large differences between the NOAA-ESRL and PSU values. The PSU value is within 0.5 ppm of the NOAA-ESRL value for 83% of the values, and 96% of the PSU values are within 1 ppm of the NOAA-ESRL values. The daytime-only percentages are similar. The difference between the daily mean PSU value and the daily mean NOAA-ESRL value (Fig. 5b) is consistently less than ±0.3 ppm. The agreement decreases somewhat throughout the study, as the overall bias during the first period is 0.01 ppm, 0.09 ppm during the second, and 0.15 ppm during the third (Fig. 5b). Based on these comparisons and the inter-system comparisons discussed in Section 2.4, we conclude that the measurements made by the systems in the regional network are precise enough and accurate enough for use in calculation of the daytime and diurnally averaged, but not annually averaged, regional CO_2 differences. This does not mean that the systems could not be used to evaluate annual-mean fluxes; utilizing the high-frequency (daily, synoptic, seasonal) CO_2 signals may make this possible (Law et al., 2002).

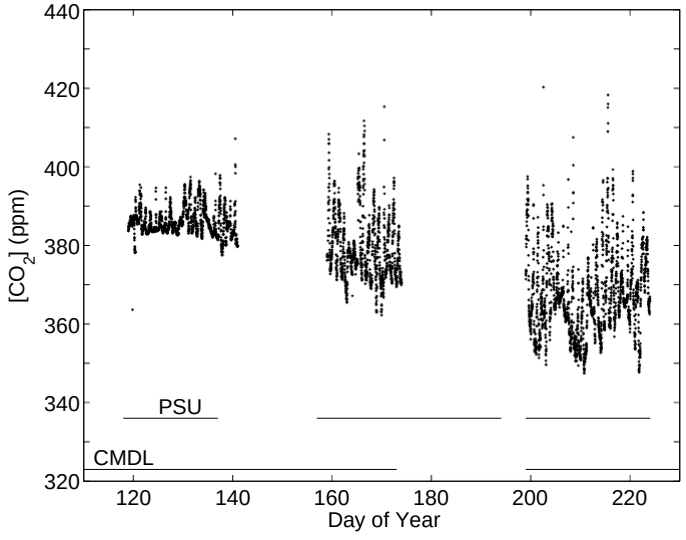

Figure 4. Time series of one-minute measurements of CO_2 mixing ratio as measured by a PSU system at the WLEF tower in northern Wisconsin during April–August 2004. Measurement height is 76 m agl. The data availability for the PSU and NOAA-ESRL systems is indicated by horizontal lines.

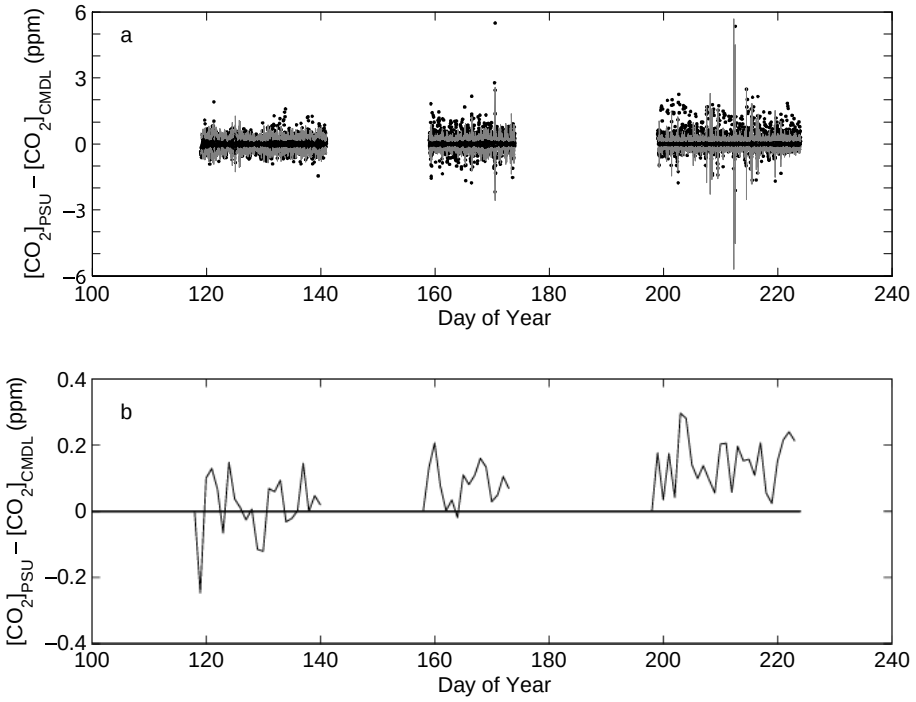

Figure 5. Difference between the CO_2 mixing ratio measured by the PSU and NOAA-ESRL systems at the WLEF tower (76-m level) during April–August 2004. a) 12-min data (solid circles) and uncertainty estimate of the NOAA-ESRL system (gray line), and b) difference between the daily average CO_2 mixing ratio measurements.

4. Field Results

4.1 Simple Lagrangian estimate of CO_2 flux

The eventual goal of this project is to use the regional network data in a full atmospheric inversion to determine the spatially- and temporally-varying regional flux. To examine the feasibility of such a task, we employ a Lagrangian model of atmospheric transport to estimate the daytime CO_2 flux on two days (11 and 20 June 2004) in which the wind direction was such that air parcels should have traveled from at least one measurement site to another, in which the wind speed was relatively constant for several hours, and in which the CO_2 concentration changed smoothly over time. A cold front passed through the region on 9 June, after which a stationary front developed near the southern boundary of Wisconsin and persisted throughout the day on 11 June. Cloudy conditions were observed throughout the day on 11 June. Following the passage of a cold front on 18 June, the skies on 20 June are mostly clear, with scattered and broken clouds,

On 11 June, the wind direction as measured at the 30-m level of the WLEF tower was 110º (southeasterly) and the wind speed at the same level averaged 6.5 m s^{-1}. WLEF was roughly downwind of Fence on that day. Although Brule was roughly downwind of WLEF as well, there was an abrupt change in the CO_2 concentration measured at Brule at 15 LST, violating our assumptions. The parcel transit times between Fence and WLEF was 2.8 hr. The change in mixing ratio between Fence and WLEF was 2−3 ppm which is large compared to the instrument accuracy. In order to calculate the flux, an estimate of the boundary layer depth is required. The Green Bay morning 1200 GMT (0600 LST) temperature sounding temperature gradient and heat fluxes from the Sylvania tower site were used to roughly estimate boundary layer depth encroachment, averaged over the time of parcel transit. The entrainment flux was assumed to be zero, which is a reasonable assumption for midday when the ABL growth is small. The boundary layer depth increased from 800 m to 950 m. We interpreted the change in mixing ratio between Fence and

WLEF as caused by ecosystem fluxes as an air parcel flows between sites. The time-averaged midday NEE of CO_2 was thus estimated to be −4 μmol m^{-2} s^{-1}.

On 20 June, the wind direction was 220º (southwesterly) and the wind speed 7 m s^{-1}. Bayfield was roughly downwind of Brule, with a parcel transit time of 2.7 hr, and Fence was roughly downwind of Wittenberg with a parcel transit time of 5.0 hr. The midday, regional average NEE estimated on 20 June, using the same Lagrangian ABL parcel assumptions was −17 μmol m^{-2} s^{-1}, considerably larger than on 11 June. We estimate the uncertainty of the Lagrangian midday mean NEE calculations, based on uncertainty in the ABL depth, transit times, and CO_2 mixing ratios, to be at least 3 μmol m^{-2} s^{-1}. For comparison, the midday average net ecosystem-atmosphere exchange (NEE) measured at 30 m on the WLEF tower was −5 μmol m^{-2} s^{-1} on 11 June and −9 μmol m^{-2} s^{-1} on 20 June. As with the fluxes we estimated, the flux was a larger magnitude on 20 June, a mostly sunny day, than on 11 June, a cloudy day. While the 122-m and 396-m data are generally used to calculate the flux during unstable atmospheric conditions (Davis et al., 2003), the data at those heights were, unfortunately, not available on 20 June. Midday fluxes at these levels typically yield NEE values that are on average larger in magnitude (more negative) than 30 m measurements by 10-20% (Davis et al., 2003; Ricciuto et al., in press). On 11 June, the flux measured at 122 m averages −6 μmol m^{-2} s^{-1} and the flux was not available at 396 m.

We do not expect our estimated fluxes for the region to agree exactly with the WLEF-measured fluxes, as the region contains different ecosystem types and the regional flux is an aggregate of the fluxes that would be measured at each tower. As noted, both Wang et al., (2006) and Desai et al., (in press a and b), find via upscaling methods that regionally aggregated NEE of CO_2 in a 40x40 km^2 region centered on the WLEF tower should show larger magnitude growing season NEE (more uptake) than is observed directly within the WLEF flux footprint. Thus this Lagrangian budget calculation finds 1) measureable differences in CO_2 across the network, as expected (Table 1); 2) the magnitude of the differences are consistent with reasonable NEE magnitudes, including less uptake of CO_2 in cloudy conditions; 3) qualitative consistency with upscaling efforts that suggest that WLEF NEE in midsummer is smaller (less uptake) than the regional average. More definitive comparison with upscaling efforts is warranted after a more complete atmospheric inverse flux estimate is completed. It is also important to note the inherent warning of the measurements from the Brule tower on 6 June that imply more complex transport and/or flux distributions than can be interpreted by our simple Lagrangian transport model. Transport from the boundary layer over Lake Superior may be involved. Our network does not include trace gas measurements that could be used to diagnose terrestrial, oceanic and anthropogenic sources or sinks. This is a weakness of our observational design that we hope is alleviated by our temporally and spatially dense sampling.

4.2.1 Case study: Frontal passage on 29 April 2004

As a further demonstration of the utility of the network, we present a case study of the CO_2 mixing ratios measured with the network on a day with a clear frontal passage. Within the regional network on 29 April 2004, all five sites (with the exception of Wittenberg) show an abrupt increase in CO_2 mixing ratio followed by a gradual decline (Fig. 6). The timing of the increase in CO_2 mixing ratio coincides with a frontal passage through the region, from the northwest to the southeast (not shown). The Brule data indicate temporarily elevated CO_2 mixing ratios immediately following each calibration sequence, which is likely a consequence of inadequate flushing of the lines. This problem is not noted at the other study sites. The front crossed the WLEF tower at 1015 GMT. Decreases in H_2O mixing ratio and temperature, and an increase in in pressure occurred as the front passed. Wind speeds decreased following the front, and the wind direction shifted from southerly to northwesterly. The skies were generally clear throughout the majority of the day, with some scattered clouds around the time of the frontal passage and overcast skies beginning late in the day (at 2000 GMT in Wausau, WI). Sunset at WLEF occurred at 0106 GMT, and sunrise at 1051 GMT.

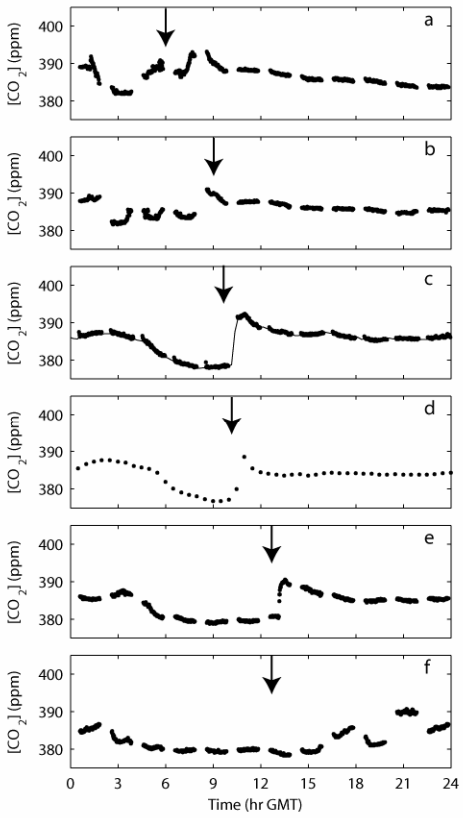

Figure 6. CO_2 mixing ratio measured at sites within the regional network for 29 April 2004. a) Brule, b) Bayfield, c) WLEF, d) Sylvania, e) Fence, and f) Wittenberg. Except for the Sylvania site, the measurement heights are 76 m and data shown are 1-min averages. At the Sylvania site, the measurement height is 36 m and the data shown are 30-min averages. Both a PSU system (dots) and a NOAA-ESRL system (line) recorded data at the WLEF tower. Arrows indicate the approximate time of frontal passage at each site (to the nearest hour) as determined from surface observations of pressure, temperature, and winds. Sunset at WLEF occurred at 0106 GMT, and sunrise at 1051 GMT.

Prior to the frontal passage the CO_2 mixing ratio measured at 76 m at WLEF decreased from 386 ppm at 0230 GMT to 377 ppm at 0830 GMT (Fig. 6). The frontal passage ocurred during a calibration cycle of the PSU system so no data were recorded during the rapid change, but the CO_2 mixing ratio immediately before the frontal passage was 379 ppm and immediately after was 391 ppm. The NOAA-ESRL system recorded two intermediate points between the prefrontal value and the postfrontal value 36 min later. Similar increases were observed at other levels by the NOAA-ESRL system. After the frontal passage, the CO_2 mixing ratio gradually fell to 386 ppm and remained relatively constant for the duration of the day.

Local surface biological fluxes are not likely to be responsible for these changes in CO_2 mixing ratio, as the observed change in CO_2 mixing ratio was very large. Typical hourly biological fluxes during the growing season are at most ±20 μmoles C m^{-2} s^{-1} (±1 ppm hr^{-1}) and during the dormant season ±2 μmoles C m^{-2} s^{-1} (±0.1 ppm hr^{-1}). In addition, leaf-out had not yet occurred in the region (based on sub-canopy photosynetically active radiation measurements, leaf-out in the area surrounding WLEF occurred around 10 May in 2004, with full expansion around 11 June, [B. Cook, personal communication]). The remaining possible explanations, horizontal and vertical advection, are investigated in Section 4.2.2 using influence functions derived from a Lagrangian Particle Dispersion (LPD) model.

4.2.2 Influence functions

To investigate possible causes for the measured trends in CO_2 mixing ratio observed during the case study we examine influence functions, which indicate the origins of the particles that affect the observed changed in mixing ratio measured at each of the towers. The influence functions were estimated using a Lagrangian Particle Dispersion (LPD) model in a receptor-oriented mode (backward in time) for each tower. The LPD model was driven by the CSU RAMS (Regional Atmospheric Modeling System) run on a single grid with a horizontal grid spacing of 20 km and nudged to NCEP reanalysis meteorological fields. The influence functions used here were calculated for a passive tracer with a constant in time surface flux.

Surface influence functions for the case study day, 29 April 2004, indicate that the source region for all the towers was to the southwest at 0000 GMT , before the front entered the region. As the front progressed, the source region for each tower switched progressively to the northwest until by 1800 GMT, the source regions for all of the towers was to the northwest (not shown). The horizontally-integrated influence functions (not shown) show the vertical structure of the source region for each tower. Before the frontal passage, the influence is confined to the boundary layer. After the frontal passage, there is influence from the free troposphere, indicating the presence of vertical mixing. For comparison, on 9 June 2004, one of the days with no fronts chosen for the simple Lagrangian flux estimation, the horizontally-integrated influence function (not shown) is relatively constant, with weak influence from the free troposphere, and a diurnal variation of the influence near the surface as the boundary layer depth changed.

While we cannot definitively determine the cause of the observed pattern in $[CO_2]$, we can use the model-derived influence functions, satellite information, and free tropospheric $[CO_2]$ measurements to present hypotheses that are consistent with the available information. The satellite-derived (NASA MODIS) normalized difference vegetation index (NDVI) (not shown) shows more greenness to the south of the study region than to the northwest, which is not surprising for late spring. Before the frontal passage at each site, the surface influence functions for 29 April 2004 indicate that the source region was south of the study region, where the growing season had begun, as judged by the normalized difference vegetation index.. Thus relatively CO_2-depleted air was advected towards the towers before the front. During and immediately after the frontal passage at each site, the source region was the north-west as indicated by the influence functions, bringing CO_2-rich air from the areas in which the vegetation was not yet active for the season, causing a large jump in CO_2 mixing ratio. After the initial jump in CO_2 as the front passed, the influence functions horizontally-integrated, showing the changes vertically in the influence functions for each site, suggest that there was increased influence from the troposphere after the frontal passage, leading to the observed gradual decline of the $[CO_2]$, in the direction of the free tropospheric value at that time (379.8 ppm for April and 380.9 ppm for May) .

These observations are similar to those of Hurwitz et al (2004), who presented case studies of several fronts observed at the WLEF tower and hypothesized that a mixture of horizontal and vertical transport but not local NEE of CO_2 was reponsible for the patterns observed during fronts. This is also similar to Wang et al., (in press) who show, using the Simple Biosphere terrestrial ecosystem model coupled to the Regional Atmospheric Modeling System, that one particularly strong CO_2 frontal event was driven primarily by horizontal transport, and that the coupled model, with boundary conditions from global-scale analyses, reproduces the observed time evolution of CO_2 mixing ratios in the few-day period surrounding the frontal event. This study is unique in that it documents the spatial coherence of this frontal event across a mesoscale domain.

6. Discussion

The two current techniques for estimating CO_2 flux, tower-based eddy covariance measurements and global-scale inversions based on sparse CO_2 mixing ratio measurements, yield results representing vastly different spatial scales and capturing different processes, and are thus impossible to compare in a way that yields definitive conclusions. As an effort to address this issue, a regional network for measuring CO_2 mixing ratios was devised, with six systems within a 150-km radius ring. The precision and accuracy of the network, based on laboratory tests and comparisons with a NOAA-ESRL system is 0.3 ppm. Diurnal and synoptic spatial gradients in CO_2 mixing ratios are readily measured with this network. The utility of the network is demonstrated in two ways: 1) by using the network CO_2 concentration measurements to

estimate the regional daytime mean NEE of CO_2, and 2) by presenting a case study involving the spatial coherence of a frontal passage through the region.

Horizontal gradients in CO_2 mixing ratio caused by net ecosystem-atmosphere exchange were measured with the regional network. These horizontal gradients will be the basis for using atmospheric budget methods to derive regional fluxes with spatial and temporal resolution fine enough to warrant comparison to the ChEAS regional flux tower network. The change in CO_2 mixing ratio of parcels traveling between sites is at least 2−3 ppm, which is large compared to the accuracy of the systems. A simple Lagrangian calculation of the regional flux was performed as a test of the concept. The flux was estimated on one cloudy day and one sunny day. The flux estimates are reasonable in sign and magnitude when compared to measurements from the ChEAS network of flux towers located in the region. This agreement indicates that the network of [CO_2] measurements will be useful in a more complex atmospheric inversion.

Over the course of the three-month deployment, many fronts passed through the network. One in particular was chosen as a case study because the source regions before and after front had much different CO_2 levels, inciting abrupt changes in the CO_2 mixing ratio measured at the network sites. Within the regional network on 29 April 2004, all six sites (with the exception of Wittenberg) show an abrupt increase in CO_2 mixing ratio followed by a gradual decline. The timing of the increase in CO_2 mixing ratio coincides with a frontal passage through the region. Similarly large changes in CO_2 over short time periods (4 ppm in 1 min in this case) have been noted in previous studies (Hurwitz et al., 2004; Wang et al., in press). This study, however, represents the first time a network of sensors captured the CO_2 mixing ratio signal of the progression of a front across a region.

Local surface biological fluxes are not likely to be responsible for these changes in CO_2 mixing ratio, as the observed change in CO_2 mixing ratio was very large compared to typical biological fluxes during the dormant season. This rules out a decrease in photosynthetic activity associated with clouds near fronts (Chan et al., 2004) as the cause of the CO_2 changes presented in this paper. Vertical mixing associated with the frontal passage is also an unlikely explanation for the sudden increase in CO_2 observed as the free tropospheric value at that time was lower than the peak value measured by the network sensors.

The modeled influence functions, satellite data, and free tropospheric CO_2 mixing ratios suggest that in this case horizontal advection is the cause of the change in CO_2 mixing ratio across front. Before the frontal passage at each site, the surface influence functions for the case study day indicate that the source region was south of the study region, where the growing season had begun, as judged by the normalized difference vegetation index. Thus relatively CO_2-depleted air was advected towards the towers before the front. During and immediately after the frontal passage at each site, the influence functions indicated the source region was to the north-west, bringing CO_2-rich air from the areas in which the vegetation was not yet active for the season, causing a large jump in CO_2 mixing ratio. After the initial jump in CO_2 and the frontal passage, the horizontally-integrated influence functions suggest that there was increased influence from the troposphere, leading to the observed gradual decline of CO_2 mixing ratio towards the free tropospheric value at that time.

Currently the global netowrk of CO_2 mixing ratio measurements is sparse and located preferentially in the marine boundary layer. Global inversions cannot be compared with tower-based eddy covariance measurements since the two techniques are sensitive to very different spatial scales. A denser network of CO_2 mixing ratio measurements over the continents as well as the oceans, combined with regional models and perhaps remotely-sensed CO_2 mixing ratios, seems necessary to bridge this gap. Information can be gained by using high frequency CO_2 mixing ratio data, relating changes in CO_2 mixing ratio to particular trajectories. While we have shown the utility of a regional network of CO_2 mixing ratio measurement systems, the next step is to use these data with a more complete description of regional atmospheric transport and to derive fluxes with spatial and temporal resolution fine enough to warrant comparison to the ChEAS regional flux tower network.

A manuscript describing these results and titled “Demonstration of a high-precision, high-accuracy CO_2 concentration measurement network for regional atmospheric inversions” (Miles, N.L., Richardson, S.J., Davis, K.J., Desai, A.R., Uliasz, M., and Denning, A.S.), is in preparation and will be submitted to the

Journal of Atmospheric and Oceanic Technology. In addition, the manuscript "Carbon flux bias estimation employing Maximum Likelihood Ensemble Filter (MLEF)" (Zupanski, D., Denning, A.S., Uliasz, M., Zupanski, M., Schuh, A.E., Rayner, P.J., Peters, W., and Corbin, K.D., to be submitted to J. Geophys. Res.) uses simulated CO_2 concentrations from the data collected during this project to evaluate the MLEF data assimilation approach to estimate biases in the CO_2 photosynthesis and respiration fluxes. Two other papers are planned as well, describing forward simulations of events during the "Ring of Towers 2004" and presenting a map of net ecosystem-atmosphere exchange for the analysis period.

9. References

Baker, I., A.S. Denning, N. Hanan, L. Prihodko, M. Uliasz, P.-L. Vidale, K.J. Davis, and P.S. Bakwin, 2003. Simulated and Observed Fluxes of Sensible and Latent Heat and CO_2 at the WLEF-TV Tower Using SiB2.5. *Global Change Biology*, **9**, 1262-1277.

Bakwin, P.S., Tans, P.P., Hurst, D.F., and Zhao, C., 1998. Measurements of carbon dioxide on very tall towers: Results of the NOAA/CMDL program, Tellus, 50B, 401–415.

Baldocchi, D., Falge, E., Gu, L., Olson, R., Hollinger, D., Running, S., Anthoni, P., Bernhofer, Ch., Davis, K., Evans, R., Fuentes, J., Goldstein, A., Katul, G., Law, B., Lee, X., Malhi, Y., Meyers, T., Munger, W., Oechel, W., Paw U, K. T., Pilegaard, K., Schmid, H. P., Valentini, R., Verma, S., Vesala, T., Wilson, K., and Wofsy, S., 2001. FLUXNET: A new tool to study the temporal and spatial variability of ecosystem-scale carbon dioxide, water vapor, and energy flux densities, Bull. Amer. Meteor. Soc., 82, 2415–2434.

Bresee, M.K., Le Moine, J., Mather, S., Brosofske, K.D., Chen, J., Crow, T.R., and Rademacher, J., 2004. Disturbance and landscape dynamics in the Chequamegon National Forest, Wisconsin, USA, from 1972 to 2001, Land. Ecol., 19 (1), 291–309.

Bousquet, P., Peylin, P., Ciais, P., LeQuere, C., Friedlingstein, P., and Tans, P., 2000. Regional changes in carbon dioxide fluxes of land and oceans since 1980, Science, 290, 1342–1346.

Chan, D., Yuen, C.W., Higuchi, K., Shashkov, A., Liu, J., Chen, J., and Worthy, D., 2004. On the CO_2 exchange between the atmosphere and the biosphere: the role of synoptic and mesoscale processes, Tellus, 56B, 194–212.

Cook, B.D., Davis, K.J., Wang, W., Desai, A.R., Berger, B.W., Teclaw, R.M., Martin, J.M., Bolstad, P., Bakwin, P., Yi, C., and Heilman, D., 2004. Carbon exchange and venting anomalies in an upland deciduous forest in northern Wisconsin, USA, Agric. Forest Meteor., 126 (3–4), 271–295.

Davis, K.J., Bakwin, P.S., Yi, C., Berger, B.W., Zhao, C., Teclaw, R.M., and Isebrands, J.G., 2003. The annual cycles of CO_2 and H_20 exchange over a northern mixed forest as observed from a very tall tower, Global Change Biol., 9 (9), 1278–1293.

Denning, A.S. et al., *Science Implementation Strategy for the North American Carbon Program.* Prepared for the Carbon Cycle Science Steering Group and the Interagency Working Group On Carbon. Available at **http://www.carboncyclescience.gov**, 2005.

Denning, A. S., Collatz, J. G., Zhang, C., Randall, D. A., Berry, J. A., Sellers, P. J., Colello, G. D., and Dazlich, D. A., 1996a. Simulations of terrestrial carbon metabolism and atmospheric CO_2 in a general circulation model, Part 1: Surface carbon fluxes, Tellus, 48B, 521–542.

Denning, A. S., Randall, D. A., Collatz, G. J., and Sellers, P. J., 1996b. Simulations of terrestrial carbon metabolism and atmospheric CO_2 in a general circulation model, Part 2: Spatial and temporal variations of atmospheric CO_2, Tellus, 48B, 543–567.

Desai, A., A. Noormets, P. V. Bolstad, J. Chen, B. D. Cook, K. J. Davis, E. S. Euskirchen, C. Gough, J. M. Martin, D. M. Ricciuto, H. P. Schmid, J. Tang, and W. Wang, In press a. Influence of vegetation type, stand age and climate on carbon dioxide fluxes across the Upper Midwest, USA: Implications for regional scaling of carbon flux. In press, *Agricultural and Forest Meteorology*.

Desai, A.R., P.R. Moorcroft, P.V. Bolstad and K.J. Davis, In press b. Regional carbon fluxes from a observationally constrained dynamic ecosystem model: Impacts of disturbance, CO_2 fertilization, and heterogeneous land cover. In press, *J. Geophysical Research Biogeosciences.*

Enting, I. G., Trudinger, C. M., and Francey, R. J., 1995. A synthesis inversion of the concentration and delta ^{13}C of atmospheric CO_2 , Tellus, 47B, 35–52.

Fan, S., Gloor, M., Mahlman, J., Pacala, S., Sarmiento, J., Takahashi, T., and Tans, P., 1998. A large terrestrial carbon sink in North America implied by atmospheric and oceanic carbon dioxide data and models, Science, 282, 442–446.

Gerbig, C., J.C. Lin, S.C. Wofsy, B.C. Daube, A.E. Andrews, B.B. Stephens, P.S. Bakwin, and C.A. Grainger, 2003. Toward constraining regional-scale fluxes of CO2 with atmospheric observations over a continent: 2. Analysis of COBRA data using a receptor-oriented framework, *Journal of Geophysical Research D: Atmospheres*, **108** (D24, 4757), (doi:10.1029/2003JD003770).

Gloor, M., Fan, S.M., Pacala, S., Sarmiento, J., 2000. Optimal sampling of the atmosphere for purpose of inverse modeling: A model study, Global Bio. Cycles, 14(1), 407–428.

Goulden, M. L., Wofsy, S. C., Harden, J. W., Trumbore, S. E., Crill, P. M., Gower, S. T., Fries, T., Daube, B. C., Fan, S.-M., Sutton, D. J., Bazzaz, A., and Munger, J. W., 1998. Sensitivity of boreal forest carbon balance to soil thaw, Science, 279, 214−218.

Gurney, K.R., Law, R.M., Denning, A.S., Rayner, P.J., Baker, D., Bousquet, P., Bruhwiler, L., Chen, Y.-H., Ciais, P., Fan, S., Fung, I.Y., Gloor, M., Heimann, M., Higuchi, K., John, J., Maki, T., Maksyutov, S., Masarie, K., Peylin, P., Prather, M., Pak, B.C., Randerson, J., Sarmiento, J., Taguchi, S., Takahashi T., and Yuen, C.-W., 2002. Towards robust regional estimates of CO_2 using atmospheric transport models, Nature, 415, 626–630.

Hurwitz, M.D., Ricciuto, D.M., Bakwin, P.S., Davis, K.J., Wang, W., Yi, C., and Butler, M.P., 2004. Transport of carbon dioxide in the presence of storm systems over a northern Wisconsin forest, J. Atmos. Sci., 61, 607–618.

Janssens, I.A., G.-J. Nabuurs, G. Folberth, B. Schlamadinger, R.W.A. Hutjes, R. Ceulemans, E.-D. Schulze, R. Valentini, A.J. Dolman, A. Feibauer, P. Ciais and P. Smith, 2003. Europe's terrestrial biosphere absorbs 7 to 12% of European anthropogenic CO_2 emissions. *Science,* **300**, 1538-1542.

Kitzis, D., and Zhao, C., 1999. CMDL/Carbon Cycle Greenhouse Gases Group standards preparation and stability. NOAA Tech. Memo ERL-14, 14 pp.

Law, R.M., Rayner, P.J, Steele, L.P., Enting, I.G., 2002. Using high frequency data for CO_2 inversions, Global Bio. Cycles, 16(4), 1053, doi:10.1029/2001G001593.

Mackay, D.S., B.E. Ewers, B,D. Cook, and K.J. Davis, Environmental drivers of evapotranspiration in a shrub wetland and an upland forest in northern Wisconsin. In press, Water Resources Research.

Masarie, K. A. and Tans, P. P., 1995. Extension and integration of atmospheric carbon dioxide data into a globally consistent measurement record, J. Geophys. Res., 100(D6), 11593–11610.

Masarie, K. A., Langenfelds, R. L., Allison, C. E., Conway, T. J., Dlugokenchy, E. J., Francey, R. J., Novelli, P. C., Steele, L. P., Tans, P. P., Vaughn, B., and White, J. W. C., 2001. NOAA/CSIRO Flask Air Intercomparison Experiment: A strategy for directly assessing consistency among atmospheric measurements made by independent laboratories, J. Geophys. Res., 106(D17), 20445−20464.

Matross, D.M., J.C. Lin, S.C. Wofsy, B.C. Daube, E.W. Gottlieb, V.Y. Chow, J.T. Lee, C. Zhao, P.S. Bakwin, J.W. Munger, D.Y. Hollinger, A. Andrews, M. Pathmathevan and C. Gerbig, 2006. Estimating regional carbon exchange in New England and Quebec by combining atmospheric, ground-based and satellite data. *Tellus B*, **58**, 344-358.

NCEP, 2004. [Available from National Climatic Data Center, Federal Building, 151 Patton Avenue, Asheville, NC 28801-5001.]

NOAA, 2004. [Available from Climate Monitoring and Diagnostics Laboratory, 325 Broadway R/CMDL 1, Boulder, CO 80305-3328.]

Pacala, S.W., Hurtt, G.C., Houghton, R.A., Birdsey, R.A., Heath, L., Sundquist, E.T., Stallard, R.F. Baker, D., Peylin, P., Ciais, P., Moorcroft, P., Caspersen, J., Shevliakova, E., Moore, B., Kohlmaier, G., Holland, E., Gloor, M., Harmon, M.E., Fan, S.-M., Sarmiento, J.L., Goodale, C., Schimel, D., and Field, C.B., 2001. Convergence of land- and atmosphere based U.S. carbon sink estimates, Science, 292, 2316–2320.

Rayner, P. J., Enting, I. G., and Trudinger, C. M., 1996. Optimizing the CO2 observing network for constraining sources and sinks. Tellus, 48B, 433−444.

Rayner, P. J., I. G. Enting, R. J. Francey, and R. Langenfelds, 1999. Reconstructing the recent carbon cycle from atmospheric CO_2, $\delta^{13}C$, and O_2/N_2 observations, Tellus, 51B, 213–232.

Ricciuto, D. M., M. P. Butler, K. J. Davis, B. D. Cook, P. S. Bakwin, A. E. Andrews, and R. M. Teclaw. Causes of interannual variability in ecosystem-atmosphere CO_2 exchange in a northern Wisconsin forest using a Bayesian synthesis inversion. In press, *Agricultural and Forest Meteorology*.

Wang, J.-W., A. S. Denning, L. Lu, I. T. Baker, K. D. Corbin, K. J. Davis, Observations and simulations of synoptic, regional, and local variations in atmospheric CO_2. In press, ***J. Geophys. Res. Atmos***.

Wang, W., K.J. Davis, B.D. Cook, M.P. Butler, and D.M. Ricciuto, 2006. Decomposing CO_2 fluxes measured over a mixed ecosystem at a tall tower and extending to a region: A case study. ***J. Geophys. Res. Biogeosci.* 111** (G02005), doi:10.1029/2005JG000093

Wofsy, S. C., Goulden, M. L., and Munger, J. W., 1993. Net exchange of CO_2 in a mid-latitude forest, Science, 260, 1314–1317.

Zhao, C.L., Tans, P., and Thoning, K.W., 1997. A high precision manometric system for absolute calibrations of CO_2 in dry air, J. Geophys. Res., 102(D5), 5885–5894.